RBF-BASED SLIDING MODE CONTROL METHOD FOR LUMBER DRYING SYSTEM

Zheng Zhou
Lecturer
Mechanical and Electrical Engineering College
Northeast Forestry University
Harbin, China
and
Electrical and Information College
Heilongjiang Bayi Agricultural University
Daqing, China
E-mail: zhouzheng_006@163.com

*Keqi Wang**
Doctor
Mechanical and Electrical Engineering College
Northeast Forestry University
Harbin, China
E-mail: zdhwkq@163.com

(Received January 2019)

Abstract. Lumber is an indispensable raw material for people's daily life. Drying process is a crucial stage in lumber manufacture. As to ensure a suitable and usable end product of lumber, most of its MC must be removed by drying. Improving the quality of lumber drying requires efficient control scheme. This article presents a design of radical basis function (RBF) neural network–based sliding mode controller for lumber drying system. RBF neural network is introduced to optimize the conventional sliding mode controller. The proposed strategy has been theoretically and experimentally investigated to demonstrate the applicability for lumber drying process. Comparative study of conventional sliding mode control (SMC) scheme and proposed control scheme is also presented. It was found that the control performance of RBF-based sliding mode controller was superior to the conventional sliding mode controller in computer simulation. Furthermore, in the field conditions, time and energy consumption reduction were noticed with RBF-based sliding mode controller compared with conventional SMC strategy using the same drying schedule, although the drying quality using the two control methods were similar.

Keywords: Lumber drying, RBF neural network, sliding mode control.

INTRODUCTION

Wood continues to be a principal raw material for a large number of products as in building construction and furniture industry (Awadalla et al 2004). Lumber drying, the final process before lumber manufacturing, is significantly crucial in forestry product industry (Yan et al 2001), for the commercial value and usability of lumber mainly depends on its drying quality. Under the same drying schedule, drying quality and energy consumption highly depends on control technique. Improving drying quality can increase lumber use efficiency and reduce waste of raw material as well. From the perspective of dry-bulb temperature and EMC control for drying kiln, lumber drying is a time delay control process with parameter uncertainties and external disturbances, which is always required for better dynamic and steady behavior.

Meanwhile, various control methodologies for lumber drying have been developed, including immune PID control (Wang and Jia 2013), intelligent fuzzy-PID control (Xiong and Wang 2012), adaptive dead-beat control (Stanislav and Radek 2015), and fuzzy logic control (Yan et al 2001). In the previous studies, PID or modified PID techniques are commonly noted

* Corresponding author

Wood and Fiber Science, 51(3), 2019, pp. 300-308
https://doi.org/10.22382/wfs-2019-028

in the field of control system for lumber drying. Nonetheless, there seems to be room for improvement in the respond time and control precision of lumber drying system. Sliding mode control (SMC) is a nonlinear control method that alters the dynamics of a nonlinear system by application of a discontinuous control signal. The past years have witnessed successful application of SMC in various areas (Wang et al 2018). A fuzzy control–based SMC method was investigated for an uncertain active suspension system (Wen et al 2017). An extended-state observer-based second-order SMC method was proposed for three-phase two-level grid-connected power converters (Liu et al 2017). SMC shows a better dynamic performance and provides fast response with regards to trajectory tracking and disturbance rejection in the recent studies (Soltanpour et al 2014; Vaidyanathan and Volos 2016; Vijay and Jena 2016; Fu et al 2019). However, the limitation of the conventional SMC controller for lumber drying can be found in the study by Zhou and Wang (2018). A chatter in the system phase locus can be noticed near the origin point, which may stimulate unstable system dynamics, degrading the overall control performance in real-time implementations.

In this study, a modified SMC, ie radical basis function (RBF)–based sliding mode controller, for lumber drying is proposed. A RBF network is an artificial neural network that uses radial basis function as activation functions. The output of the network is a linear combination of radial basis functions of the inputs and neuron parameters. RBF neural network is a universal approximator (Cheng et al 2009), which has been widely used to solve nonlinearities and uncertainties for complex system (Cheng et al 2008; Cheng et al 2010). Control parameters play a crucial role for system stability and dynamic performance of the switching function. RBF neural network is concerned in approximating the SMC output and compensating the disturbance. The switching function is considered as the input of the RBF neural network in RBF-SMC. To demonstrate the feasibility and validity of the proposed strategy, numerical simulations and experimental results has been carried out in the study.

The remainder of this article is organized as follows. Section 2 builds the lumber drying model and presents the RBF-SMC control scheme. Section 3 illustrates the simulation results. Experiment results are demonstrated in Section 4. Finally, conclusions are derived in Section 5.

SLIDING MODE CONTROLLER DESIGN

Description of Lumber Drying Model

Modeling and control strategies for lumber drying were widely shown in previous literature. An extensive number of computing models have been developed (Hasanand Langrish 2016; Berner et al 2017; Zadin et al 2015), which generally aimed at explaining the physical phenomenon during drying, such as water migration, heat distribution, etc. However, too many inputs exploited to build theoretical models make it difficult to integrate with real-time predictive control system. To simplify the lumber drying model, mathematical method such as artificial neural networks and support vector machines have also been used to build drying model because of their ability of capturing nonlinearities (Ge and Chen 2014; Nadian et al 2015). Because of the feasible predicting of the performance for lumber drying process, the method of autoregressive model with exogenous inputs (ARX) is used to describe the system in this study. The ARX model specifies that the output variables depend linearly on their own previous values and are stochastic; thus, the model is in the form of a stochastic difference equation. A computational model of lumber drying process that integrated flexibility is presented. Ignoring the constant velocity of air blowing through the surface of the lumber sample, lumber MC during drying mainly depends on the dry-bulb temperature and EMC (Zadin et al 2015). Hence, the MC and EMC were taken as outputs of the control system. Because the dry-bulb temperature and EMC are controlled by three valves, ie heater, sprayer, and damper, installed in the drying kiln; the opening degree of the three valves was taken as input variables of the prediction model.

The second-order ARX model built to describe the lumber drying process is defined as follows:

$$\begin{aligned} y(t) = & -a_1 y(t-1) - a_2 y(t-2) \\ & + b_{11}u_1(t-1) + b_{12}u_1(t-1) \\ & + b_{21}u_2(t-1) + b_{22}u_2(t-2) \\ & + b_{31}u_3(t-1) + b_{32}u_3(t-2) \\ & + v(t), \end{aligned} \tag{1}$$

where, $y(t)$, $u(t)$, and $v(t)$ are output, inputs, and disturbance of the model, respectively. a_1, a_2, b_{mn} ($m = 1\ldots3, n = 1, 2$) represent the coefficients for the respective input variables.

Eq (1) can be rewritten in the matrix form as

$$y(t) = \varphi^{\mathrm{T}}(t)\theta + v(t), \tag{2}$$

where θ is the coefficient vector and $\varphi(t)$ is the information matrices. θ is obtained using RLS algorithm. Eq (2) can be simply written as follows:

$$Y_t = H_t\theta + V_t. \tag{3}$$

The quadratic criterion function is defined using least squares identification principle:

$$J(\theta) := V_t^{\mathrm{T}} V_t = (Y_t - H_t\theta)^{\mathrm{T}}(Y_t - H_t\theta). \tag{4}$$

According to the quadratic criterion function, Eq (5), which is the RLS estimation of ARX parameter vector θ is obtained. In the ARX wood-drying process model, the initial value of $P^{-1}(t)$ is $P^{-1}(0) = P_0^l$, $\cdot p^0 = 10^6$,

$$\begin{aligned} &\hat{\theta}(t) = \hat{\theta}(t-1) + P(t)\varphi^{\mathrm{T}}(t)\left[y(t) - \varphi^{\mathrm{T}}(t)\hat{\theta}(t-1)\right], \\ &P^{-1}(t) = P^{-1}(t-1) + \varphi(t)\varphi^{\mathrm{T}}(t), P(0) + P_0^l > 0. \end{aligned} \tag{5}$$

RBF-SMC Controller Design

Equivalent controller design. In this part, a discrete-time sliding mode controller combined with an RBF compensator is presented. The second-order linear computational model built in 2.1 describing the dry-bulb temperature and EMC for lumber drying is written as follows:

$$x(k+1) = A_1\mathrm{x}(k) + B_1\mathrm{u}(k) \tag{6}$$

where

$$x(k) = \left[x^1(k), x^2(k)\right]^{\mathrm{T}}.$$

Transform the discrete Eq (6) into discrete error-state Eq (7), defined as follows:

$$x_e(k+1) = A_e x_e(k) + B_e u(k) + f(k), \tag{7}$$

where

$$\begin{aligned} f(k) &= \begin{bmatrix} -r(k) - A_{12}\dot{r}(k) + r(k+1) \\ A_{22}r'(k) + \dot{r}(k+1) \end{bmatrix} \\ &= R_1 - A_1 R, R = [r(k)\mathrm{d}r(k)]^{\mathrm{T}}, \\ R_1 &= [r(k+1)\,\mathrm{d}r(k+1)]^{\mathrm{T}}. \\ A_e &= A_1, B_e B_1, x_e = [e(k)\,\mathrm{d}e(k)]^{\mathrm{T}}. \end{aligned}$$

Here, $r(k)$ is position function, and its change rate is $\mathrm{d}r(k)$; $e(k)$ is error, and its change rate is $\mathrm{d}e(k)$; $e(k)$ and $\mathrm{d}e(k)$ are expressed as follows:

$$e(k) = r(k) - x_1(k), \mathrm{d}e(k) = \mathrm{d}r(k) - x_2(k). \tag{8}$$

The switching function of sliding mode controller is characterized as follows:

$$s(k) = ce(k) + \mathrm{d}e(k) = Cx_e(k), \tag{9}$$

where $C = [c\ 1]$.

Using Eqs (7) and (9), we get

$$\begin{aligned} s(k+1) &= Cx_e(k+1) \\ &= CA_e x_e(k) + C[B_e u(k) + f(k)]. \end{aligned} \tag{10}$$

According to Eqs (9) and (10), the equivalent controller is obtained:

$$u_{\mathrm{eq}}(k) = -(Cb)^{-1}[C(A_e - I)x_e(k) + Cf(k)]. \tag{11}$$

RBF algorithm is adopted to improve the robustness of the system, the RBF-SMC control law is designed as follows:

$$u(k) = u_{\text{eq}}(k) + u_n(k), \tag{12}$$

where $u_n(k)$ is the output of the RBF neural network.

RBF controller design. The Gaussian function is given by

$$h_j = \exp\left(-\frac{\|X - C\|^2}{ab_j^2} \right), j = 1, 2\cdots, m, \tag{13}$$

where $X = [x_1 x_2 \cdots x_n]^T$ is the network input, $H = [h_1 h_2 \cdots h_j \cdots h_m]^T$ is output of the network hidden layer, $C_j = [c_{j1} \cdots c_{jm}]^T$ and $b_j = [b_{j1} \cdots b_{jm}]^T$ are the center vector and width vector of the jth neuron in the RBF network, respectively, and m is the number of hidden layer.

The weight vector yields

$$W = \left[w_1 w_2 \cdots w_j \cdots w_m \right]^T. \tag{14}$$

The output of the RBF neural network is

$$u_n(k) = w_1 h_1 + w_2 h_2 + \cdots + w_m h_m. \tag{15}$$

The two inputs of the RBF network are

$$x_n(1) = s(k), \tag{16}$$

$$x_n(2) = s(k) - s(k-1). \tag{17}$$

The RBF network learning index is defined in

$$E(k) = \frac{1}{2} s^2(k). \tag{18}$$

From Eqs (7) and (9), we can get

$$\frac{\partial s(k)}{\partial u_n(k)} = \mathrm{B}_e(2). \tag{19}$$

The weight, the center vector, and the width vector of the RBF network output are given by

$$\begin{aligned} \Delta w_j &= -\frac{\partial E(k)}{\partial w_j} = -s(k) \frac{\partial s(k)}{\partial u_n(k)} \frac{\partial u_n(k)}{\partial w_j} \\ &= -s(k) \mathrm{B}_e(2) h_j, \end{aligned} \tag{19}$$

$$\begin{aligned} w_j(k) &= w_j(k-1) + \eta \Delta w_j \\ &\quad + \alpha \left[w_j(k-1) - w_j(k-2) \right], \end{aligned} \tag{20}$$

$$\begin{aligned} \Delta b_j &= -\frac{\partial E(k)}{\partial b_j} = -s(k) \frac{\partial s(k)}{\partial u_n(k)} \frac{\partial u_n(k)}{\partial b_j} \\ &= -s(k) \mathrm{B}_e(2) w_j h_j \frac{\left\| x_n - C_j \right\|}{b_j^3}, \end{aligned} \tag{21}$$

$$\begin{aligned} \Delta c_{ji} &= -s(k) \frac{\partial s(k)}{\partial u_n(k)} \frac{\partial u_n(k)}{\partial c_{ji}} \\ &= -s(k) \mathrm{B}_e(2) w_j \frac{x_{nj} - c_{ji}}{b_j^2}, \end{aligned} \tag{22}$$

$$\begin{aligned} c_{ji}(k) &= c_{ji}(k-1) + \eta \Delta c_{ji} \\ &\quad + \alpha \left[c_{ji}(k-1) - c_{ji}(k-1) \right]. \end{aligned} \tag{23}$$

Here, η is learning rate, α is inertia coefficient.

SIMULATION RESULT

In this section, the computer simulations are conducted to validate the feasibility and effectiveness of the proposed RBF-SMC strategy. MATLAB® was used to simulate the control curves of dry-bulb temperature and EMC of lumber drying process. As the dry-bulb temperature and EMC in each stage of the drying schedule is different, the given position tracking adopted step command. RBF-SMC controllers with different key parameters were used to control the system in multiple experiments, which are carried out in Figs 1-3. The simulation of RBF-SMC controllers for dry-bulb temperature and EMC are exhibited in Figs 4 and 5, which were compared with the conventional SMC method. In this case, three aspects of control performance are considered, one was the response time of reaching the set reference signal, one was the overshoot of the control curve, and the other involved the ability to track the set-point.

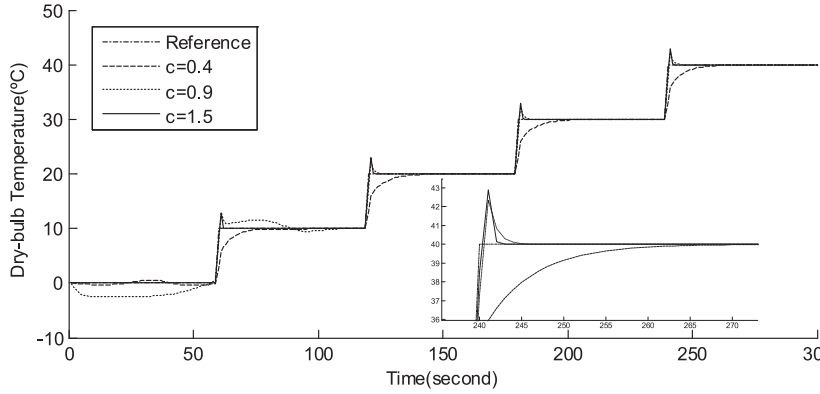

Figure 1. Simulation response of dry-bulb temperature with different c.

Figure 1 shows the results of the dry-bulb temperature position tracking in the condition of RBF-SMC control with $c = 0.4$, $c = 0.9$, and $c = 1.5$ ($\eta = 0.1$, $\alpha = 0.5$). As shown in Fig 1, the response curve with $c = 0.4$ has no overshoot, and the adjusting time is the longest among the three control responses. As regard to overshoot, response time, and the stability of the system, the parameters with $c = 0.9$ and $c = 1.5$ provides better control performance than $c = 0.4$. The response time with $c = 1.5$ is shorter than $c = 0.9$; however, the overshoot with $c = 1.5$ is larger than $c = 0.9$.

Figure 2 illustrates the simulation results of RBF-SMC controllers for dry-bulb temperature with $\eta = 0.1$, $\eta = 0.8$, and $\eta = 1.2$ ($c = 0.9$, $\alpha = 0.5$). Among the three controllers, the controllers with $\eta = 0.1$ and $\eta = 1.2$ achieve better dynamic performance than the controller with $\eta = 1.2$. The steady-state error is zero with $\eta = 0.1$ and $\eta = 1.2$, an obvious chattering can be observed in the early 180 s with $\eta = 0.8$. The controller presents the smallest overshoot with $\eta = 0.8$ and largest with $\eta = 1.2$. The system response has a shortest adjusting time with $\eta = 0.8$ and longest with $\eta = 0.1$.

Figure 3 depicts the simulation results of dry-bulb temperature controllers with $\alpha = 0.1$, $\alpha = 0.5$, and $\alpha = 0.9$ ($c = 0.9$, $\eta = 0.1$). It is manifested that the response ability improved with the decrease of α; the average stable time with $\alpha = 0.1$ is the shortest and $\alpha = 0.9$ is the longest. However, chatter

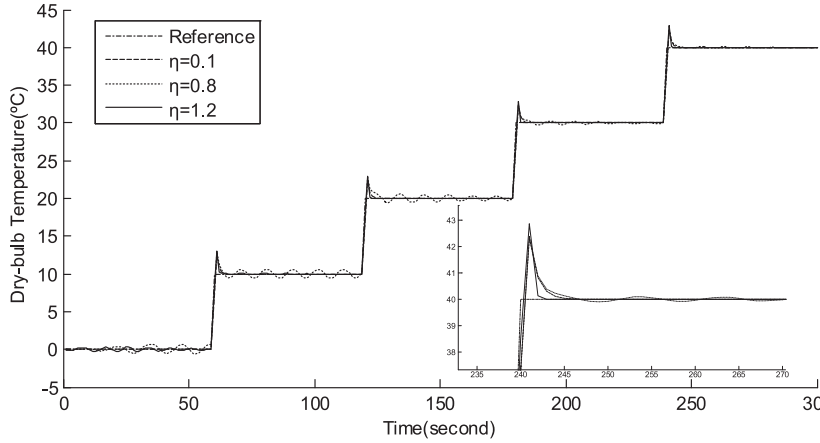

Figure 2. Simulation response of dry-bulb temperature with different η.

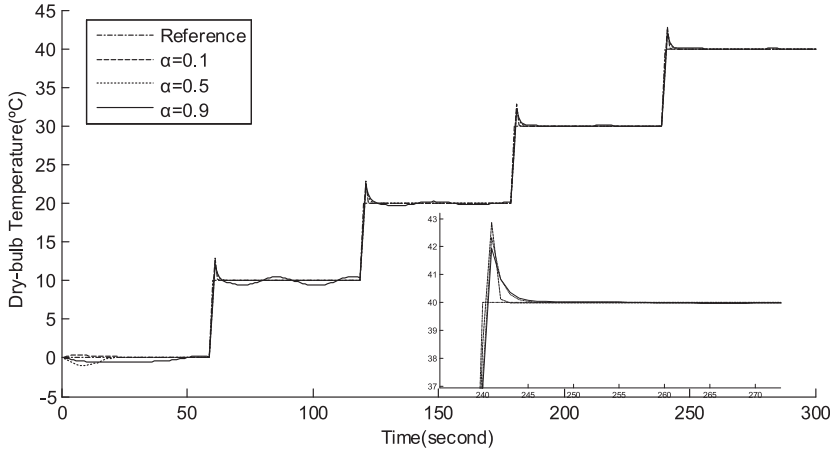

Figure 3. Simulation response of dry-bulb temperature with different α.

occurs with the increased value of α, especially in the early 180 s. The overshoot intends oppositely to the response speed; the control curve with $\alpha = 0.9$ has the smallest overshoot and $\alpha = 0.1$ has the largest. Figures 1-3 demonstrate that the proposed method can precisely follow the reference signal.

Figures 4-5 demonstrate the simulation response of dry-bulb temperature and EMC via RBF-SMC method, which are compared with the tracking performance of the conventional SMC algorithm. The control parameters and indices of dry-bulb temperature and EMC controllers are shown in Tables 1 and 2, in which the response time and overshoot are compared. As shown in Fig 4, the RBF-SMC method leads to a more rapid tracking response than SMC. The average overshoot of RBF-SMC for the proposed method is 12.2%, whereas that value for SMC is 48.13%. From Fig 5, there is no overshoot of SMC; the average overshoot of RBF-SMC is 1.75%. The average response times of RBF-SMC and SMC are 2.25 s and 24 s, respectively. The results imply that the RBF-SMC achieves a better dynamic performance with a tolerant overshoot and fast response than the SMC controller.

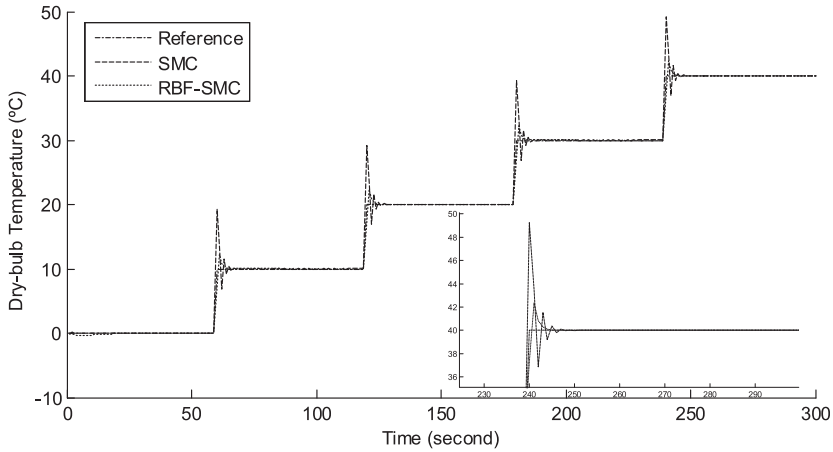

Figure 4. Simulation response of dry-bulb temperature.

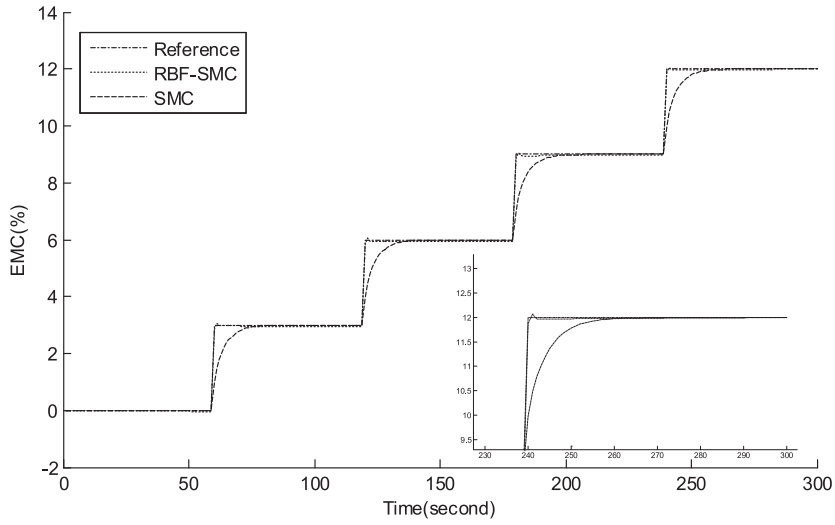

Figure 5. Simulation response of EMC.

EXPERIMENTAL RESULTS

In this section, experimental results are obtained to test the performance of the proposed RBF-SMC strategy, which is also compared with SMC controllers. The experimental material was Japanese cedar (*Cryptomeria japonica* D. Don); size of the lumber sample was 2100 mm × 120 mm × 30 mm, the average initial MC was around 70%, and the average density was about 0.334 g/cm^3. The whole drying experiment included two stages, air-seasoning and kiln drying, and the study focused on the control method for kiln drying stage.

Dry-bulb temperature and EMC were the average of the values measured by six temperature sensors and six humidity sensors installed in the drying kiln. Figure 6 shows the dry-bulb temperature and MC curves via RBF-SMC compared with SMC. The drying of the wood samples via RBF-SMC and SMC, both starting with an initial dry-bulb temperature with 40°C and finishing as 90°C, took a total time of 46 h and 41 h, respectively, which is also indicated in Table 3. As far as the energy cost is concerned, the electricity consumption adopting RBF-SMC controller had 59 kWh reduction compared with SMC. The initial MC of SMC and RBF-SMC kiln drying process were 13.84% and 13.47%. After the kiln drying stage, the final MC of SMC and RBF-SMC were found to be 7.28% and 6.66%, respectively.

The specific indices of the MC are shown in Table 3, in which drying time, average final MC standard, mean square error (MSE) of MC, and the quality standard are presented. According to

Table 1. Control indices of dry-bulb temperature RBF-SMC and SMC controllers.

	Response time (s)		Overshoot (%)	
Reference (°C)	RBF-SMC	SMC	RBF-SMC	SMC
10	7	11	23.3	92.1
20	7	11	11.7	46.3
30	7	11	7.8	30.9
40	7	11	5.8	23.2
Average	7	11	12.2	48.13

RBF, radical basis function; SMC, sliding mode control.

Table 2. Control indices of RBF-SMC and SMC controllers.

	Response time (s)		Overshoot (%)	
Reference (%)	RBF-SMC	SMC	RBF-SMC	SMC
3	2	24	3.3	—
6	2	24	1.7	—
9	2	24	1.1	—
12	3	24	0.9	—
Average	2.25	24	1.75	—

RBF, radical basis function; SMC, sliding mode control.

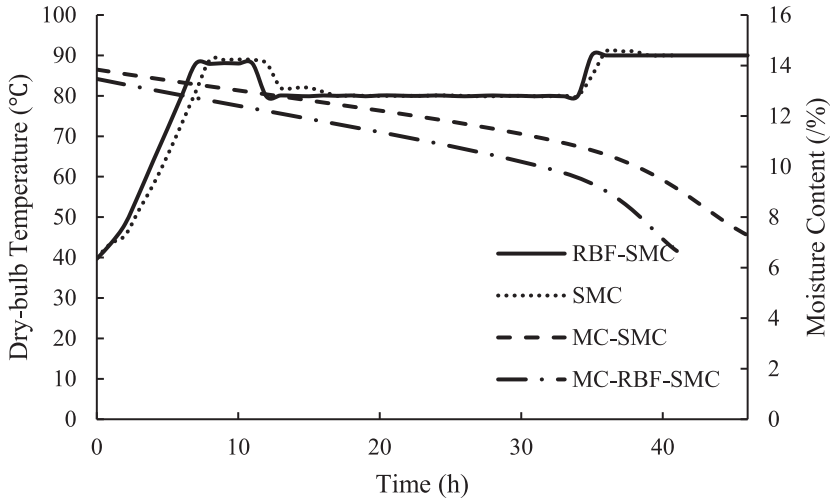

Figure 6. Dry-bulb temperature and MC curves of RBF-SMC and SMC controllers.

China National Standards of Drying Quality of Sawn Timber (GB/T6491-2012), the average MC of RBF-SMC and SMC have achieved first-class and second-class MC standard, respectively. MSEs of MC are 0.32% and 0.20% via SMC and RBF-SMC strategy, respectively; both achieved the first-class MSE standard. Statistics of MC deviation and residual stress of the lumber samples are shown in Table 4. The MC deviation and average residual stress of the lumber sample drying in the condition of SMC and RBF-SMC method achieve first-class standard. Visible flaws, including surface checks, internal checks, end checks, color changing, and collapse, are shown in Table 5. The drying process via SMC, surface checks, end checks, and collapse were found in 2%, 2%, and 4% of the total samples, and internal checks and color changing was not found. As for the drying process used RBF-SMC, end checks and collapse both occurred in 2% in the lumber samples, and there was no surface checks, internal checks, and color changing.

The indexes shown in Tables 3-5, which are applied to evaluate the quality of lumber drying process, indicated that the same (first) class was achieved for both of RBF-SMC and SMC. However, better results were obtained with RBF-SMC algorithm, especially in terms of drying time, energy consumption, and final MC.

CONCLUSIONS

Sliding mode control algorithm combined with RBF neural network is demonstrated in this lumber drying system study. The proposed method is verified by simulation and experiment results. Influence of RBF parameters on system control behavior was examined. Dynamic and steady-state performance with the proposed control scheme was studied, which demonstrates that the proposed method can precisely follow the

Table 3. Statistical results of MC.

Algorithm	Drying time (h)	Average final MC (%)	Average final MC standard	MSE (%)	MSE standard
SMC	46	7.28	II	0.32	I
RBF-SMC	41	6.66	I	0.20	I

RBF, radical basis function; SMC, sliding mode control; MSE, mean square error.

Table 4. MC deviation and residual stress of the lumber samples.

Algorithm	Average MC deviation (%)	MC deviation standard	Average residual stress (%)	Average residual stress standard
SMC	1.33	I	0.42	I
RBF-SMC	1.50	I	0.41	I

RBF, radical basis function; SMC, sliding mode control.

Table 5. Visible flaw.

Algorithm	Surface checks	Internal checks	End checks	Color changing	Collapse
SMC	2%	none	2%	none	4%
RBF-SMC	none	none	2%	none	2%

RBF, radical basis function; SMC, sliding mode control.

reference signal. The optimal RBF parameters for lumber drying system in this study was $c = 0.9$, $\eta = 0.1$, and $\alpha = 0.5$. The simulation comparison between RBF-SMC and conventional SMC indicates that the proposed method led to a more accurate tracking result and faster convergence than conventional SMC scheme. In field experience, the proposed technique had a better performance with regard to the final MC, drying time, and energy consumption, although the drying quality was similar.

ACKNOWLEDGMENTS

This work was financially supported by the University Nursing Program for Young Scholars with Creative Talents in Heilongjiang Province (NO. UNPYSCT-2018083).

REFERENCES

Awadalla HSF, El-Dib AF, Mohamad MA, Reuss M, Hussein HMS (2004) Mathematical modelling and experimental verification of wood drying process. Energy Convers Manage 45(2):97-207.

Berner MO, Sudbrock F, Viktor Scherer V, Mönnigmann M (2017) POD and Galerkin-based reduction of a wood chip drying model. International Federation of Automatic Control 50(1):6619-6623.

Cheng L, Hou ZG, Tan M, Lin Y, Zhang W (2010) Neural-network-based adaptive leader-following control for multiagent systems with uncertainties. IEEE Trans Neural Netw 8(21):1351-1358.

Cheng L, Hou ZG, Tan M (2008) A neutral-type delayed projection neural network for solving nonlinear variational inequalities. IEEE Trans Circuits Syst, II Express Briefs 55(8):806-810.

Cheng L, Hou ZG, Tan M (2009) Adaptive neural network tracking control for manipulators with uncertain kinematics, dynamics and actuator model. Automatica 45(10): 2312-2318.

Zhang D, Cao J, Sun L (2010) Dynamic modeling of wood drying process based on SLSSVM. Pages 431-435 in IEEE International Conference on Computer Science and Information Technology, July 9-11, 2010.

Fu L, Tola E, Al-Mallahi A, Li R, Cui Y (2019) A novel image processing algorithm to separate linearly clustered kiwifruits. Biosyst Eng 183:184-195.

Ge L, Chen GS (2014) Control modeling of ash wood drying using process neural networks. Optik (Stuttg) 125(22): 6770-6774.

Hasan M, Langrish TAG (2016) Time-valued net energy analysis of solar kilns for wood drying: A solar thermal application. Energy 96:415-426.

Liu J, Vazquez S, Wu L, Marquez A, Gao H, Franquelo LG (2017) Extended state observer-based sliding-mode control for three-phase power converters. IEEE Trans Ind Electron 64(1):22-31.

Nadian MH, Rafiee S, Aghbashlo M, Hosseinpur S, Mohtasebi SS (2015) Continuous real-time monitoring and neural network modeling of apple slices color changes during hot air drying. Food Bioprod Process 94:263-274.

Soltanpour MR, Khooban MH, Khalghani MR (2014) An optimal and intelligent control strategy for a class of nonlinear systems: Adaptive fuzzy sliding mode. J Vib Control 22(1):159-175.

Stanislav P, Radek M (2015) Application of adaptive dead-beat controller in drying process. Procedia Eng 100:756-764.

Vaidyanathan S, Volos C (2016) Advances and applications in nonlinear control systems. Springer International Publishing, New York, NY. 15 pp.

Vijay M, Jena D (2016) Intelligent adaptive observer-based optimal control of overhead transmission line de-icing robot manipulator. Adv Robot 30(17-18):1215-1227.

Wang H, Jia H (2013) Study of immune PID controller for wood drying system. Pages 827-831 in IEEE International Conference on Communication Systems and Network Technologies, April 6-8, 2013.

Wang Y, Gao Y, Karimi HR, Shen H, FangZ (2018) Sliding mode control of fuzzy singularly perturbed systems with application to electric circuit. IEEE Trans Syst Man Cybern Syst 48(10):1667-1975.

Wen S, Chen, MZQ, Zeng Z, Yu X, Huang T (2017) Fuzzy control for uncertain vehicle active suspension systems via dynamic sliding-mode approach. IEEE Trans Syst Man Cybern Syst 47(1):24-32.

Xiong MC, Wang LL (2012) Intelligent fuzzy-PID temperature controller design of drying system. Pages 54-57 in International IEEE Conference on Information Management, Innovation Management and Industrial Engineering, October 20-21, 2012.

Yan GCK, Silva CWD, Wang XG (2001) Experimental modelling and intelligent control of a wood-drying kiln. Int J Adapt Control Signal Process 15(8):787-814.

Zadin V, Kasemagi H, Vigonski V, Vigonski S, Veske M, Aabloo A (2015) Application of multiphysics and multiscale simulations to optimize industrial wood drying kilns. Appl Math Comput 267:465-475.

Zhou Z, Wang K (2018) Sliding mode controller design for wood drying process. Wood Sci Technol 52(4):1039-1048.